Scale dependence of the coarse-grained velocity derivative tensor structure in turbulence

Aurore Naso and Alain Pumir*

Institut Non Linéaire de Nice (UMR CNRS 6618), Université de Nice Sophia Antipolis, 1361 Route des Lucioles, F-06560 Valbonne, France

(Received 18 August 2005; published 17 November 2005)

Velocity fluctuations in hydrodynamic turbulence have a nontrivial structure, characterized by correlations of the velocity gradient tensor. In this paper, we consider a phenomenological model, incorporating the main features of hydrodynamic fluid turbulence, aimed at predicting the structure of the velocity gradient tensor M coarse grained at a spatial scale r. This model [M. Chertkov, A. Pumir, and B.I. Shraiman, Phys. Fluids **11**, 2394 (1999)] is formulated as a set of stochastic ordinary differential equations, with three dimensionless parameters, characterizing the reduction of the nonlinearity induced by the pressure term, the reisotropization effect of the small scale velocity field, and the influence of the small scales on the coarse-grained velocity derivative tensor. Semiclassical solutions of this model are obtained and compared with direct numerical simulations (DNS) data. The DNS data show that the joint probability distribution function of the second and third invariants of M becomes increasingly skewed as the scale r decreases in the inertial range. The model results correctly reproduce this behavior provided the parameter that controls nonlinearity reduction is finely tuned; the influence of the other parameters in the model is much weaker.

DOI: 10.1103/PhysRevE.72.056318 PACS number(s): 47.27.Eq, 47.27.Gs, 02.70.Rr, 05.10.Gg

I. INTRODUCTION

The seemingly random velocity fluctuations observed in a turbulent fluid motion are characterized by their spatial correlations. These correlations are responsible for the power law dependence of the energy spectrum, described by the Kolmogorov K41 theory [1]. Generally, it has proven fruitful to investigate spatial scaling properties of various velocity correlation functions, and in particular its deviations from the K41 theory [2]. One of the major limitations of these studies, however, is that the connection with the dynamical (Navier-Stokes) equations remains somewhat weak. The line of research pursued in this article is aimed at developing a better understanding of scaling properties, based on dynamical considerations [3].

The recent work on advection of a passive scalar by a turbulent flow [4] provides much inspiration and guidance for our present effort. As it is the case for the velocity field, the passive scalar exhibits strong deviations from K41 theory. A clear understanding of this problem has emerged from the study of simple models, such as the Kraichnan model [5] or other models [6]. The seemingly oversimplifying assumptions that allow one to solve the model still preserve the main physical aspects of the real solution [7,8]. From a technical point of view, these models have pointed to the importance of Lagrangian considerations.

The importance of the vorticity $\vec{\omega}=\vec{\nabla}\times\vec{u}$ to understand the dynamics of velocity fluctuations has been stressed many times [9–11]. Vorticity is essentially the antisymmetric part of the velocity gradient tensor

$$(m-m^t)/2=\begin{pmatrix} 0 & \omega_3 & -\omega_2 \\ -\omega_3 & 0 & \omega_1 \\ \omega_2 & -\omega_1 & 0 \end{pmatrix},$$

where ω_i is the component of the vorticity in the ith direction. The strain, defined as the symmetric part of the velocity derivative tensor $S\equiv(m+m^t)/2$, determines the local stretching of material lines, and of vorticity itself [12]. The velocity gradient tensor is therefore of crucial importance to understand the dynamics of turbulence.

Coarse graining of the velocity gradient tensor over a region of scale r, by defining $M_{ab}=(1/V)\int_\Gamma m_{ab}d^3x$, where Γ is a region of characteristic size r, provides an averaged description of the velocity gradient tensor at scale r, very appropriate in a number of contexts, for example, in describing the energy transfer in turbulence [13], or more generally in Large Eddy Simulations (LES) [14]. Scaling laws are expected in the description of the coarse-grained matrix M as a function of scale.

To understand the dynamics of the matrix M, one must address the question of the (Lagrangian) evolution of the volume Γ, advected by the flow. Our model couples in an essential way the evolution of the coarse-grained velocity gradient M and the geometry of the volume, represented by the moment of inertia tensor g of Γ. The problem can be posed as a set of stochastic differential equations [3]. Alternatively, the description of the system can be recast as a Fokker-Planck equation for the probability distribution function of (M,g) as a function of time t. We focus here on the properties of statistically steady state turbulent flow, so we look for stationary solutions of the Fokker-Planck equations. Observing that the statistics are essentially gaussian at scale larger than the integral scale provides a boundary condition for the Fokker-Planck equation, which allows us to write an explicit, although completely formal solution as a path integral [3].

*Electronic address: Alain.Pumir@inln.cnrs.fr

To proceed any further requires a numerical evaluation of this path integral. In view of the complexity of the problem, we consider here a semiclassical solution of the problem. This approach is a significant improvement, compared to the very simplified approach used in Ref. [3], consisting of estimating the path integral by taking only the deterministic solution. The semiclassical approach accounts for the fluctuations in a more systematic manner. The search for the minimal action trajectory in the appropriate parameter space is not a straightforward task. The solution used here is based on a combination of simplex method (amoeba algorithm), coupled with a Monte Carlo procedure. The latter is necessary to escape from numerous relative extrema.

Our results have been presented in the plane of the invariants of the matrix M [the (R,Q) plane [3,15]], which leads to a synthetic presentation of the topology of the flow. The results of the model can be compared with the results of direct numerical simulations (DNS), obtained at moderate Reynolds number ($R_\lambda=130$), presented here, as well as with the results of experiments [14]. These results provide an important constraint in the study of this model.

The model is introduced in Sec. II. The description in terms of the (R,Q) plane is discussed in Sec. III, along with our DNS results. In Sec. IV, our method of resolution is presented. Section V is devoted to the results of this study. Finally, Sec. VI presents our concluding remarks.

II. DERIVATION AND DEFINITION OF THE MODEL

In this section, we briefly recall the derivation of the model, and introduce our notation as well as the key parameters in the model. We formulate the model here in terms of the matrix M, defining the coarse-grained velocity derivative, and the moment of inertia tensor g characterizing the geometry of the Lagrangian volume. Our model describes the Lagrangian evolution of M and g in terms of the following set of equations:

$$\frac{dM}{dt} + (1-\alpha)(M^2 - \Pi \mathrm{Tr}(M^2)) = \eta, \tag{1}$$

$$\Pi \equiv g^{-1}/\mathrm{Tr}(g^{-1}), \tag{2}$$

$$\frac{dg}{dt} - gM - M^t g - \beta\sqrt{\mathrm{Tr}(MM^t)}\left(g - \frac{1}{3}\mathrm{Tr}(g)Id\right) = 0, \tag{3}$$

$$\langle \eta_{ab}(\rho;t)\eta_{cd}(0;0)\rangle = \gamma\left(\delta_{ac}\delta_{bd} - \frac{1}{3}\delta_{ab}\delta_{cd}\right)\frac{\varepsilon}{\rho^2}\delta(t), \tag{4}$$

where $\rho^2=\mathrm{Tr}(g)$. Aside from the dimensional quantity ε, the energy dissipation, the model involves three dimensionless parameters α, β, and γ.

To justify these phenomenological equations, it is convenient to consider a tetrahedron of Lagrangian particles, whose positions are $\vec{r}_i$ $(i=1-4)$. Because of the assumed homogeneity of the flow, the motion of the center of mass $\vec{\rho}_0 = \Sigma_i \vec{r}_i$ is imaterial, so the geometry of the tetrad is described by a set of three reduced coordinates, $\vec{\rho}_i$. It is more convenient to define the tensor ρ_i^a where a is the spatial index, and the moment of inertia tensor $g=\rho^t\rho$.

The evolution equation for the coarse-grained velocity derivative tensor M is reminiscent of the evolution equation for the velocity gradient tensor $m_{ab}\equiv\partial_a u_b$: $dm/dt+m^2=H$, where H is the pressure Hessian, plus viscous corrections. Numerical observations [3,16] indicate that the pressure term tends to diminish the nonlinear effect: $H\sim\alpha m^2$, where the parameter α in Eq. (1) parametrizes the reduction of the nonlinearity. The incompressibility condition, $\mathrm{Tr}(M)=0$ is satisfied, thanks to the $\Pi\mathrm{Tr}(M^2)$ term [$\mathrm{Tr}(\Pi)=1$, by construction]. This choice of Π as a "projection operator" to impose incompressibility is dictated by the fact that (i) the pressure term does not do any work, as it should be the case in an incompressible flow, and (ii) in the deterministic case ($\eta=0$), the solutions of the system do not blow-up in a finite time. The stochastic term represents the effect of the rapidly fluctuating small scales on the pressure term. It is assumed to be gaussian, white in time, with a scaling form as a function of spatial scales compatible with Kolmogorov scaling. The dimensionless factor γ simply measures the intensity of this noise term.

The equation describing the evolution of the moment of inertia tensor (the "geometry") of the set of points, Eq. (3), can be understood by decomposing the velocity field as an overall, shape preserving displacement, a straining flow, coherent over the scale ρ [$\mathrm{Tr}(g)=\rho^2$] of the object, and an incoherent, fluctuating component of the velocity field. Each of these three terms can be formally written by a filtering of the velocity field. The global displacement is ignored here, as we are considering an homogeneous flow. The straining term is responsible for the coupling between M and g in Eq. (3). One way to model the incoherent part of the velocity field over the set of points is to add a fluctuating, white in time noise term, as proposed in Refs. [3,17]. The effect of such a term would be (i) to contribute to the overall growth of the object and (ii) to counteract the tendency of the stretching term gM to generate very anisotropic shapes [17]. We have simply replaced the noise term by the β term in Eq. (3). This term effectively tends to restore the isotropy of the geometry. This simplifies the search of solutions, as we will explain below.

To summarize, our model reduces to a set of stochastic differential equations. In addition to the dimensional parameter ε, the rate of energy dissipation, it involves three dimensionless parameters: α, the reduction of nonlinearity, β, the tendency for the small scale fluctuations to restore isotropy of the shape, and γ, the strength of the noise term in the M equation. One of the objectives of this work is to explore the qualitative solutions of the model in terms of these three parameters.

III. DIAGNOSTICS

A. The (R,Q) plane

Before presenting the results of the model, we explain in what way the velocity gradient tensor M enables a precise diagnostics of the flow topology. In the incompressible case,

its three eigenvalues can be expressed as a function of the two invariants Q and R defined as $Q=-\frac{1}{2}\mathrm{Tr}(M^2)$ and $R=-\frac{1}{3}\mathrm{Tr}(M^3)$ [15]. The local topology of the flow qualitatively depends on the sign of the discriminant $D=27R^2+4Q^3$. Thus, for $D>0$, two eigenvalues of M are complex conjugate: the flow is elliptic, with locally swirling streamlines. For $D<0$, the three eigenvalues of M are real: in that case the flow is locally hyperbolic, and strain dominates. The zero discriminant line plays a crucial role in this diagram. It has been observed that in the case of the velocity derivative tensor m, the probability distribution function is very skewed, and extends along the positive R side of the zero discriminant (PRZD) line [15], a fact viewed as a qualitative signature of dynamical effects present in a very simplified model [18]. One of the main goals of this article is to compute the joint probability distribution function of the Q, R invariants as a function of scale. We stress that this quantity can be computed in Direct Numerical Simulations of turbulence, and is now accessible in experiments [14], suggesting challenging comparisons between theory and experiments.

B. DNS results

Before presenting the results of the model, we turned to numerical simulations to obtain detailed numerical information, for comparison purposes. Briefly, we have used a standard pseudo spectral code, described in Ref. [19]. The run discussed here has a 256^3 resolution. We have made sure that the highest wave number in the simulation $k_{\max}$ is large enough to describe the smallest length scales in the flow: $k_{\max}\eta \geqslant 1.4$. Our Reynolds number is $R_\lambda=130$, and the ratio between the integral scale and η is $L/\eta \sim 100$. Because the end of the inertial range is at a scale $\sim 10\eta$, the inertial range in our simulation corresponds roughly to a factor 10 in scale.

Figure 1 shows the joint probability distribution function in the (R,Q) plane, computed at different values of the scale r in the inertial range. At the integral scale L, the distribution is almost symmetric with respect to the $R=0$ axis. As the value of r decreases, the distribution becomes stretched towards the $R>0$ part of the separatrix. It is worth noting that the asymmetry observed numerically is building up rather slowly as the scale r decreases. The probability distribution function of (R,Q) obtained when r is in the dissipative scale, $r\sim\eta$, is much more asymmetric than the one corresponding to inertial scales ($r=L/8$). This leads us to the conclusion that the dissipative effects, not included in our model, are responsible for the significant increase of asymmetry of the probability distribution function in the (R,Q) plane, in particular of the large probability built up along the PRZD line. The probability distribution functions computed from our model should thus be compared with the ones shown in Figs. 1(a)–1(d), *not* with the one computed when r is in the dissipative range, shown in Fig. 1(e)

The energy transfer in an eulerian reference frame can be readily expressed with the help of our (Lagrangian) model, Eqs. (1)–(4). In the case of isotropic tetrahedra, this energy transfer reduces to $-\alpha r^2\mathrm{Tr}(M^2M^t)$ [3,20]. In the following, we will refer to the quantity $-r^2\mathrm{Tr}(M^2M^t)$ as the energy transfer.

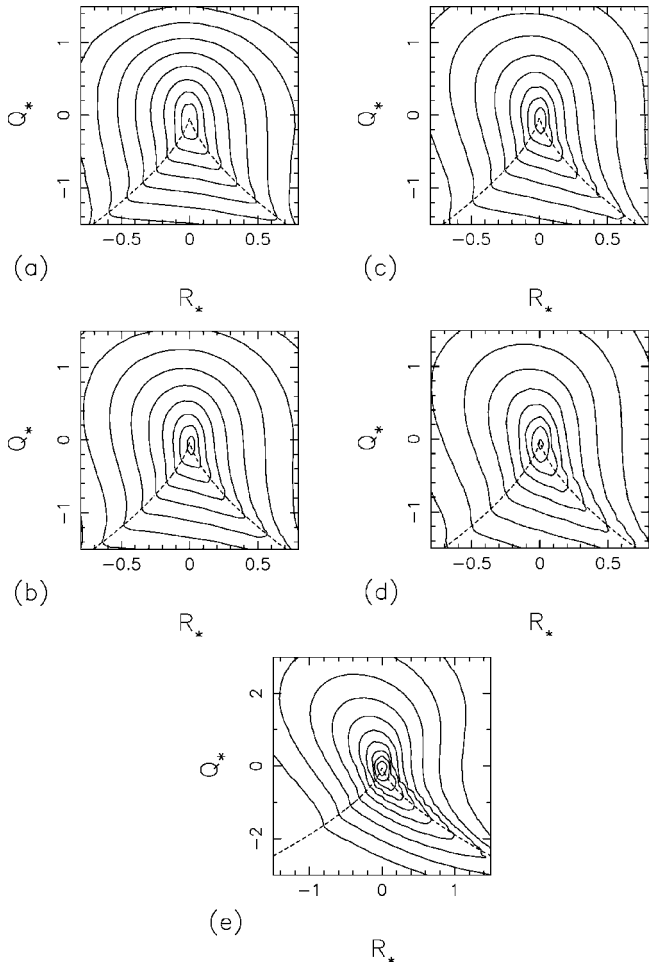

FIG. 1. PDF of Q_*,R_* invariants normalized to the variance of strain $Q_*=Q/\langle S^2\rangle$, $R_*=R/\langle S^2\rangle^{3/2}$, calculated by DNS. (a) $r=L$, (b) $r=L/2$, (c) $r=L/4$, (d) $r=L/8$, (e) $r=2\eta$. The isoprobability contours are logarithmically spaced, and separated by factors of e.

Figure 2 shows the scaling laws of the second moments of strain and vorticity, and of the energy transfer divided by r^2, $-\mathrm{Tr}(M^2M^t)$. According to the Kolmogorov scaling $\langle\Delta v(r)\rangle \propto r^{1/3}$, $M(r)$ should evolve as $r^{-2/3}$, hence the second moments of the strain S (symmetric part of M) and of the vorticity ω (antisymmetric part of M) should behave as $r^{-4/3}$, whereas the third moments behave similar to the quantity related to the energy transfer $-\mathrm{Tr}(M^2M^t)$ should behave as r^{-2}. This is consistent with the fact that the energy transfer $-r^2\mathrm{Tr}(M^2M^t)$ is independent of r in the inertial range. Figure 2 demonstrates that the Kolmogorov's predictions correctly describe the low moments of M.

IV. METHOD OF RESOLUTION OF THE SYSTEM: PATH INTEGRAL REPRESENTATION AND SEMICLASSICAL APPROXIMATION

A. Path integral representation

The system (1)–(4) defines a well-posed stochastic problem. The solutions of the problem can be conveniently studied by noticing that the probability distribution function

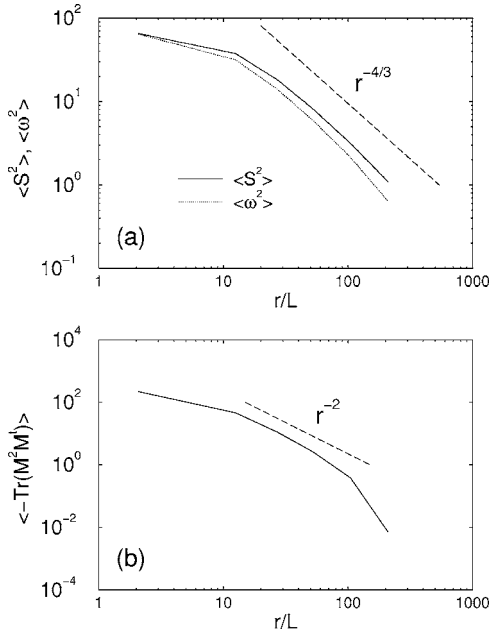

FIG. 2. Scaling laws of (a) the second moments of strain and vorticity, and (b) of the energy transfer divided by r^2, calculated by DNS.

$P(M,g,t)$ obeys a Fokker-Planck equation of the form

$$\partial_t P(M,g,t) = LP(M,g,t), \tag{5}$$

where L is a differential operator. In this article we restrict ourselves to the simplest problem of statistically steady state turbulent flows, so we simply take $\partial_t \to 0$. The system thus reduces to a (parabolic) partial differential equation in the (g,M) variables

$$LP = 0. \tag{6}$$

To solve this equation, one needs to specify the proper boundary conditions. At the largest scales of the flow, the velocity field has been shown many times to have a probability distribution function that is very close to a gaussian distribution. We use this property, and simply assume that at the integral scale, L, the probability distribution function of the matrix M is Gaussian:

$$P(M,\mathrm{Tr}(g) = 3L^2) \sim \exp\left[- \frac{\mathrm{Tr}(MM^t)}{(\varepsilon L^{-2})^{2/3}} \right]. \tag{7}$$

The solution of the Fokker-Planck equation (6) can be considered as a eulerian probability distribution function provided that the following normalization condition is imposed:

$$\int dM P(M,g) = 1. \tag{8}$$

This system can be formally solved by using Green's function methods. The Green's function has an appealing path integral formulation, in terms of all the trajectories connecting the initial point (M',g') at time $-T$ to the final point (M,g) at time 0. One obtains [3]

$$P(M,g) = \int dM' \int dT G_{-T}[M;g|M';\mathrm{Tr}(g') = 3L^2] \times P[M',\mathrm{Tr}(g') = 3L^2], \tag{9}$$

$$G_{-T}(M;g|M';g') = \int_{M(-T)=M'}^{M(0)=M} [\mathcal{D}M''] \times \int_{g(-T)=g'}^{g(0)=g} [\mathcal{D}g''] \exp[-S(M'';g'')], \tag{10}$$

$$P(M,g) = \int dM' \int dT \int_{M(-T)=M'}^{M(0)=M} [\mathcal{D}M''] \int_{g(-T)=g'}^{g(0)=g} [\mathcal{D}g''] \exp - [S(M'';g'') + \mathrm{Tr}(M'M'^t)/(\varepsilon L^{-2})^{2/3}], \tag{11}$$

$$S = \int_0^T dt \frac{\mathrm{Tr}\left([\dot{M} + (1-\alpha)(M^2 - \Pi \mathrm{Tr}(M^2))][\dot{M} + (1-\alpha)(M^2 - \Pi \mathrm{Tr}(M^2)]^t \right)}{2\gamma\varepsilon/\rho^2}. \tag{12}$$

The boundary condition (7) has been explicitely taken into account in Eqs. (9)–(11). The probability distribution function $P(M,g)$ is thus determined by considering all the trajectories starting at some time $-T<0$ with the condition that $\mathrm{Tr}(g')=3L^2$, and ending up at time=0 at (g,M). The action S provides the statistical weight of each trajectory. A proper evaluation of the probability distribution function $P(M,g)$ requires an integration over all the possible trajectories. This can be done in principle by using a Monte Carlo algorithm. However, because of the large spatial dimension, the problem seems excessively difficult. A straightforward Monte Carlo calculation leads to configurations that have widely different statistical weights (by many orders of magnitude). Understanding the origin of the statistically significant contributions to the path integral in Eq. (11) is a prerequisite to carry out a reliable Monte Carlo calculation of the solutions. The study of the semiclassical solutions presented in this article is the natural first step in such an endeavor.

A very simplified solution, consisting in ignoring completely the fluctuation term, was considered in Ref. [3]. The resulting "classical approximation" leads to solutions that reproduce in a crude manner the main features of the solutions

obtained in DNS of the Navier-Stokes equations at moderate resolution [3], and with experimental results [14].

B. Semiclassical approximation

The semiclassical approximation is obtained by identifying the trajectory that maximizes the integrand in Eq. (11). Formally, this procedure is exact in the limit where the noise term becomes small: $\gamma \to 0$. In this approximation, one simply replaces in Eq. (11) the integral by the saddle point value, obtained by substituting the "optimal trajectory" into the action term

$$P(M,g) \sim \exp - \left(S_c(M;g|M';g') + \frac{\mathrm{Tr}(M'M'^t)}{(\epsilon L^{-2})^{2/3}} \right). \quad (13)$$

The determination of the optimal trajectory can be carried out by writing the appropriate Euler-Lagrange variational equation

$$\frac{d}{dt}\frac{\partial \mathcal{L}}{\partial \dot{M}_{ab}} = \frac{\partial \mathcal{L}}{\partial M_{ab}}, \quad (14)$$

where $\mathcal{L}$ is the Lagrangian of the system ($S = \int dt \mathcal{L}$). Its expression is given in Eq. (12).

In our calculations, aimed at determining the probability distributions in the (R,Q) plane as a function of scale, the Euler-Lagrange equation (14) requires a number of *a priori* unknown boundary conditions. Specifically, imposing (R,Q) at scale r leaves three unknown free parameters to completely determine the matrix M. In addition, the time derivative of M, $\dot{M}$ is *a priori* unknown, which leaves eight extra free parameters [incompressibility imposes that $\mathrm{Tr}(\dot{M})=0$], leaving a 11-dimensional space to fully determine the initial condition. For each value of (R,Q), our approach consists in computing the logarithm of the probability distribution in Eq. (13) as a function of the 11 other parameters, and looking for its maximum.

C. Optimization methods

Our first attempt to solve the optimization problem in the 11-dimensional space of initial conditions was based on the simplex method "amoeba," which is known to converge when the function to be minimized has simple convexity properties [21]. In the problem considered here, however, the function to be optimized turns out to have a much more complicated structure, so the amoeba converged towards one of the (many) local minima of the function, but never to the searched global minimum. This difficulty can be tackled by using a combination of the simplex algorithm, and of simulated annealing techniques. The algorithm amoeba [21] was used in our work. The procedure we employed is the following: for each value of (Q,R,r) (r being the scale), an initial regular simplex of characteristic size 0.2 is considered. This object undergoes a first annealing, whose initial temperature is equal to 7, then two others, whose initial temperatures equal $yb/4$, yb being the optimal value of the function obtained in the previous annealing. In these three annealings, the temperature is decreased quadratically, and for 10 regularly spaced values of it the amoeba algorithm is iterated 300 times. In the calculations performed here, the algorithm considers that a local minimum has been found when the relative difference between the largest and the smallest values of the function over the simplex is less than 10^{-3}.

V. RESULTS AND DISCUSSION OF THE SEMICLASSICAL CALCULATIONS

The method described in the previous section to compute the "semiclassical" solutions of the model leads to a numerically tractable algorithm, that allows us to study the behavior of the solutions as a function of the three parameters α (the reduction of nonlinearity), β (the isotropizing effect of the small scale velocity fluctuations), and γ (the amplitude of the noise acting on M). The DNS results, discussed in Sec. III B, provide a natural point of comparison to discuss our data.

Our main finding in this section is that the parameter α plays the most significant role in determining the qualitative feature of the solution. Imposing that the solution exhibits the right behavior for the moments of the vorticity, the strain, and the energy transfer, as well as for the probability distribution function considerably restricts the value of α.

A. Scaling properties

We discuss first the scaling properties of quantities such as the square of the strain $\langle S^2 \rangle$ and of the vorticity $\langle \omega^2 \rangle$, as well as of the energy transfer term $\langle -r^2 \mathrm{Tr}(M^2 M^t) \rangle$.

Figure 3 shows the dependence of $\langle S^2 \rangle$ and $\langle \omega^2 \rangle$ as a function of scale for several values of α, at fixed values of β and γ ($\beta=0.4, \gamma=0.25$). The general aspect of the curves shown in Fig. 3 is essentially independent of the precise values of β and γ. The expected scaling law dependence $r^{-4/3}$ of $\langle \omega^2 \rangle$ is correctly observed for all the values of α. But the quantity that is the most sensitive to the value of α is $\langle S^2 \rangle$. The fit of the dependence of $\langle S^2 \rangle$ as a function of r by a power law shows a good agreement with the $-4/3$ exponent for $\alpha \sim 0.5$, but significant deviations from it for other values of α [see Fig. 5(a)]. This suggests that the semiclassical solutions of the model can only be compatible with the DNS data provided the value of α is large enough: $\alpha \gtrsim 0.4$.

Figure 4 shows the dependence of the energy transfer term divided by r^2, $\langle -\mathrm{Tr}(M^2 M^t) \rangle$ as a function of r at a fixed value of β and γ ($\beta=0.4$ and $\gamma=0.25$), and for various values of α. As it was the case for the quadratic quantities $\langle S^2 \rangle$ and $\langle \omega^2 \rangle$, we found that the qualitative behavior shown in Fig. 4 is fairly independent of the precise values of β and γ. The main observation is that the value of the transfer has the correct sign $\langle -r^2 \mathrm{Tr}(M^2 M^t) \rangle > 0$ provided the value of α is small enough: $\alpha \lesssim 0.5$ [see Fig. 5(b)]. For values of α in this range, we find that the energy transfer scales with the proper scale dependence, as seen in DNS. For certain values of α, the energy transfer is negative at large scales and positive at small scales: in this case we have plotted in Fig. 5(b) the average of the sign at the different scales considered. Figure 5 leads to the conclusion that the range of values of α that lead to a good qualitative agreement with the DNS results is strongly constrained: only values of α close to 0.45 (0.4

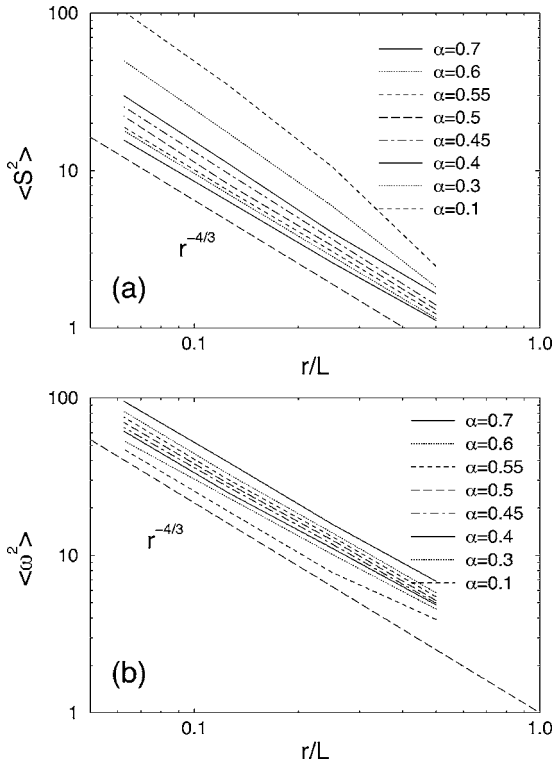

FIG. 3. Scaling laws of the second moments of (a) strain and (b) vorticity, for different values of α (β=0.4, γ=0.25). Aside from the straight line $r^{-4/3}$, α=0.7,0.6,0.55,0.5,0.45,0.4,0.3,0.1 from bottom to top in (a) and from top to bottom in (b).

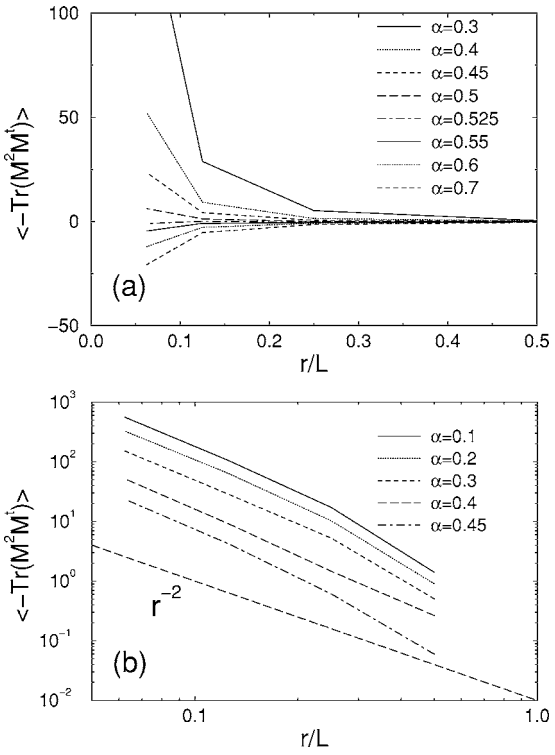

FIG. 4. The energy transfer divided by r^2, $\langle -\mathrm{Tr}(M^2M^t)\rangle$ as a function of scale r for different values of α (β=0.4, γ=0.25): (a) linear scale, (b) logarithmic scale. For large values of α this quantity is negative.

$\lesssim\alpha\lesssim$0.5) produce results qualitatively comparable to our DNS results.

B. Evolution of the probability distribution function in the (R,Q) plane

The fact that the value of α needed to obtain the right scaling of energy transfer, strain, and vorticity from the solutions of our model has to be rather precisely tuned can be also seen by studying the computed probability distribution functions in the (R,Q) plane. [Figures 6(a)–6(d)] show the probability distribution function at a large (small) value of α: α=0.6 (α=0.2), at two values of r: $r=L/2$ and $r=L/16$. The main difference between the evolution at the value α=0.6 [Figs. 6(a) and 6(b)] and at the low value α=0.2 [Figs. 6(c) and 6(d)] concerns the growth of the probability distribution along the PRZD line (the zero discriminant line is shown in dashed in Figs. 6 and 7). At small values of α, Figs. 6(c) and 6(d), the tail along the PRZD line grows considerably when the scale r decreases, significantly more than what is observed in DNS. In the other case [higher values of α, Figs. 6(a) and 6(b)] the growth of probability along the PRZD-line is not observed at all: in fact, the probability tends to grow more in other parts of the (R,Q) plane.

Figure 7 shows the density of strain [7(a)], vorticity [7(b)] and energy flux [7(c)] in the (R,Q) plane at the value α =0.5, and with β=0.4 and γ=0.25, at a value of $r=L/8$. Generally, the trends are consistent with the DNS results [3], except perhaps for the density of strain, that tends to be less concentrated around the origin compared to the DNS. Overall, the main conclusion is that the parameter α, which controls the reduction of the nonlinearity, has a very strong influence on the growth of the probability distribution along the PRZD-line: the smaller α, i.e., the stronger the nonlinear term is, the larger the tail of the probability distribution function along the PRZD line.

C. Discussion

The growth of the PDF tail along the PRZD-line predicted by the model for small values of α is generally consistent with the results of [14]. In this work, it was noticed that the small scales of the flow tend to slow down the effect of the nonlinearity, estimated at the given scale. This is precisely the origin of the α term in our model [3]. A large enough value of the parameter α is needed to sufficiently reduce the growth of the probability along the PRZD line as r decreases, consistent with the model's results.

The fact that the strain density is large in the neighborhood of the PRZD line, and that the tail seems to grow very strongly when α decreases is consistent with the fact that the strain $\langle S^2\rangle$ grows faster when r decreases at small values of α. The energy transfer is positive near this neighborhood, which explains why the value of α needs to be small enough

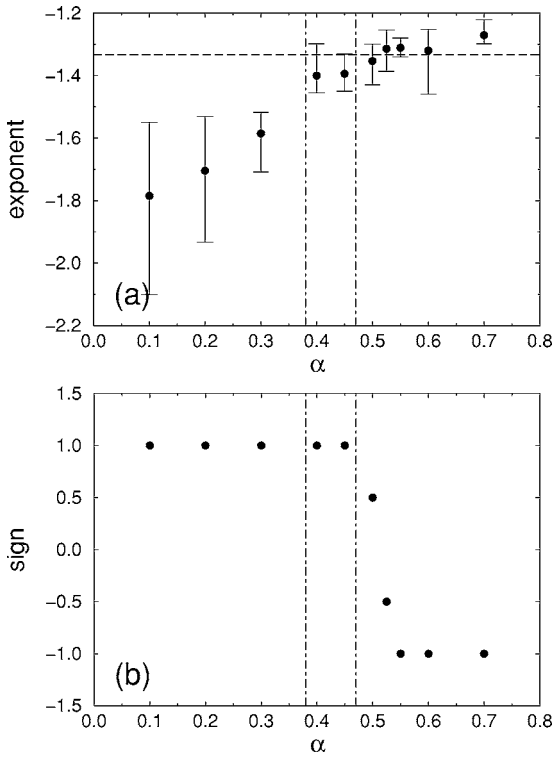

FIG. 5. Dependance with respect to α of (a) the scaling law exponent of $\langle S^2 \rangle$ and (b) the sign of the energy transfer $\langle -r^2 \mathrm{Tr}(M^2 M^t) \rangle$ (β=0.4, γ=0.25). In (a) the dashed line indicates the Kolmogorov prediction $-4/3$. In (b) is plotted for each value of α the average of the sign of the energy transfer at the different scales considered. The range of values of α leading to a qualitatively acceptable behavior of the model's solutions is delimited by the vertical dot-dashed lines.

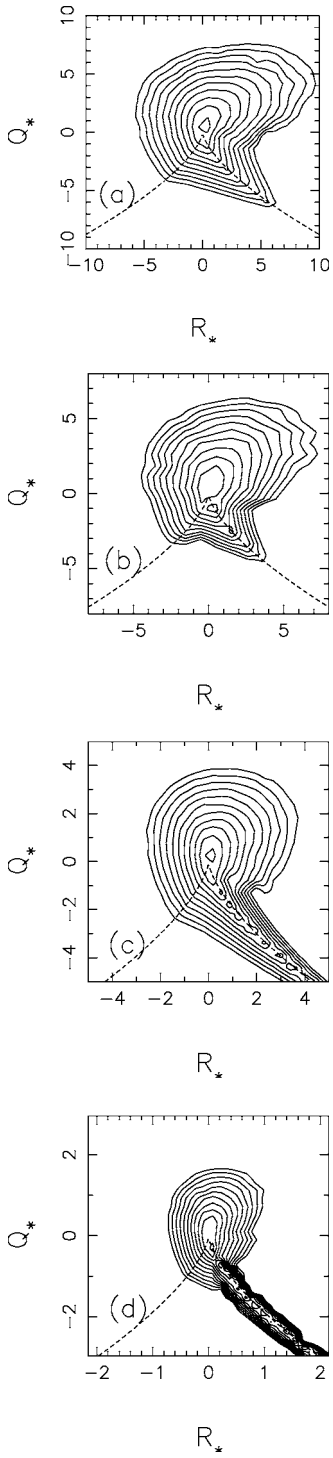

FIG. 6. PDF of Q_*, R_* invariants normalized to the variance of strain for (a) and (b) α=0.6, (c) and (d) α=0.2. (a) and (c) $r=L/2$, (b) and (d) $r=L/16$; β=0.4 and γ=0.25. The isoprobability contours are logarithmically spaced and separated by factors of e.

to have the appropriate sign of the energy transfer. Too large a value of α leads to a too small contribution from the tail along the PRZD-line, and to an improper sign of the energy transfer; whereas too small a value of α leads to an excessive growth of the strain $\langle S^2 \rangle$ at smaller scales (see Fig. 5). The enstrophy density, which is concentrated in the upper part of the (R,Q) plane, is not influenced by the tail along the PRZD-line, which is consistent with the fact that the dependance of $\langle \omega^2 \rangle$ with respect to α is much weaker.

We insist on the fact that the general picture we have illustrated here for a particular set of values of β and γ does not depend, qualitatively, on the precise value of β and γ chosen. In fact, the precise value of β plays almost no role, provided β is not very small. The strength of the noise, measured by the value of γ, plays a stronger role, although it does not affect in a significant way neither the 'transition' we observed, nor in fact the precise value of α for which the transition occurs. As an example, Fig. 8 shows the dependence of the mean values of S^2, ω^2 and $-\mathrm{Tr}(M^2 M^t)$ as a function of r for several values of γ, at fixed α and β.

Although the semiclassical solutions computed here reproduce qualitatively many features observed in the DNS and in experiments, they also show a number of inappropriate features. The most visible example, as one compares the probability distribution functions obtained from DNS and from the semiclassical solution concerns the anomalously large probability predicted in the $R>0$, $Q>0$ sector of the (R,Q) plane. This aspect of the semiclassical solutions is in quantitative disagreement with the solutions obtained by DNS, or observed experimentally [14].

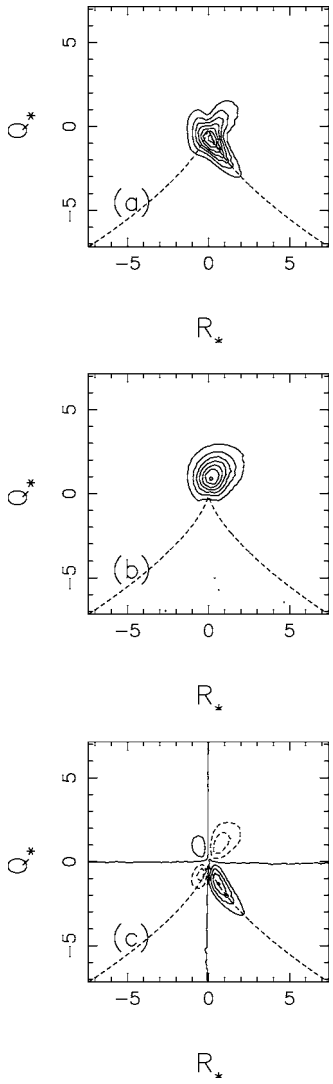

FIG. 7. (a) Strain variance, (b) enstrophy, and (c) energy flux densities in the R_*, Q_* plane for $r=L/8$, $\alpha=0.5$, $\beta=0.4$, and $\gamma=0.25$. Solid lines correspond to positive values, dashed lines to negative ones.

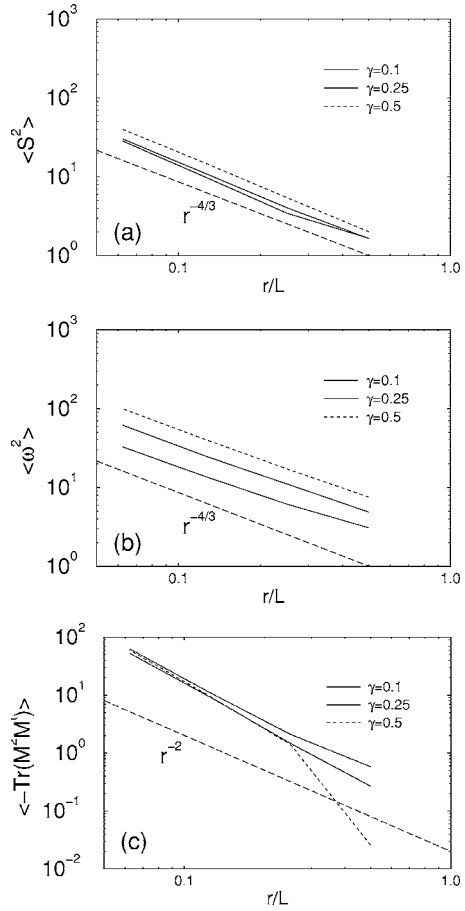

FIG. 8. Scaling laws of the second moments of (a) strain, (b) vorticity, and (c) of the energy transfer divided by r^2 for different values of γ ($\alpha=0.4$, $\beta=0.4$).

VI. CONCLUSION

We have considered a model that aims at predicting the statistical properties of the coarse-grained velocity gradient tensor M as a function of the spatial scale r. This model includes in an essential way many qualitative important features identified in turbulent flows. The model is formulated as a set of stochastic differential equations, and involves in the form considered here three dimensionless parameters α, the strength of the nonlinearity reduction, β, the amplitude of the term that restores isotropy of the tetrad, and γ, the amplitude of the noise term in the M equation. Although it is relatively easy from a technical point of view to write a formal solution in terms of path integrals, that can lead in principle to a numerical (Monte Carlo) treatment, we had to content ourselves as a first step with a semiclassical treatment, which amounts to find the largest contribution to the path integral solution of the model.

From a turbulence point of view, we have observed in DNS that the probability distribution function in the (R,Q) plane when the coarse-graining scale r is in the inertial range develops an asymmetry towards the $R>0$ part of the separatrix relatively slowly. The very skewed probability distribution functions observed in the inertial range are mostly due to a viscous (dissipative) effect, not included in our model.

Comparing the results of our model, both in terms of probability distribution function shape in the (R,Q) plane, as well as in terms of low order moments, such as $\langle S^2\rangle$, $\langle\omega^2\rangle$, and $\langle -\mathrm{Tr}(M^2M^t)\rangle$ (the energy transfer term divided by r^2), leads to important constraints on the possible values of the parameters of the model. The parameter that was found to play the most crucial role is α, which parameterizes the reduction of the nonlinearity in the model. The main effect of α is to modify the growth of the probability tail, along the separatrix. The behavior predicted by the model is in qualitative agreement with the (moderate) growth of the probability tail observed in the inertial range in DNS only for a limited range of α: $\alpha\sim 0.45$. We note that this value of α is not inconsistent with the values of α reported in the past [3,16]. In contrast, the other parameters, β and γ, do not appear to modify very significantly the qualitative behavior of the solution, unless they are extremely small (β) or too large (γ).

Although the semiclassical solutions of the model reproduce in several essential ways the probability distribution

function in the (R,Q) plane obtained by DNS, they lead to a number of quantitative incorrect features. The main example is the enhanced probability distribution in the $R>0$, $Q>0$ quadrant. The method of resolution (semiclassical) discussed here should ultimately be improved. It is our belief that the knowledge gained in obtaining semiclassical solutions should help us in designing better approximations schemes. Preliminary results in this direction are encouraging.

We also note that the model can be extended to study flows with more complicated large scale structures, such as shear [22] or contractions [23], by simply modifying the large scale boundary condition. Such detailed comparisons will provide stringent tests on the validity of our approach.

ACKNOWLEDGMENTS

We acknowledge many fruitful discussions with M. Chertkov and B. Shraiman. This work has been supported by the European Commission (Contract No. HPRN-CT-2002-00300). We acknowledge the support of IDRIS for computer time. We also acknowledge the Center for NonLinear Studies, where part of this work has been done.

[1] A. N. Kolmogorov, C. R. Acad. Sci. URSS **30**, 301 (1941).
[2] U. Frisch, *Turbulence: The Legacy of AN Kolmogorov* (Cambridge University Press, Cambridge, 1995).
[3] M. Chertkov, A. Pumir, and B. I. Shraiman, Phys. Fluids **11**, 2394 (1999).
[4] G. Falkovich, K. Gawedzki, and M. Vergassola, Rev. Mod. Phys. **73**, 913 (2001).
[5] R. H. Kraichnan, Phys. Fluids **10**, 1417 (1967).
[6] B. I. Shraiman and E. D. Siggia, C. R. Acad. Sci., Ser. IIa: Sci. Terre Planetes **321**, 279 (1995).
[7] L. Mydlarski, A. Pumir, B. I. Shraiman, E. D. Siggia, and Z. Warhaft, Phys. Rev. Lett. **81**, 4373 (1998).
[8] A. Celani and M. Vergassola, Phys. Rev. Lett. **86**, 424 (2001).
[9] E. Siggia, J. Fluid Mech. **107**, 375 (1981).
[10] S. Douady, Y. Couder, and M. E. Brachet, Phys. Rev. Lett. **67**, 983 (1991).
[11] J. Jimenez, A. Wray, P. Saffman, and R. Rogallo, J. Fluid Mech. **255**, 65 (1993).
[12] G. K. Batchelor, *An Introduction to Fluid Dynamics* (Cambridge University Press, Cambridge, 1967).
[13] S. Chen, R. E. Ecke, G. L. Eyink, X. Wang, and Z. Xiao, Phys. Rev. Lett. **91**, 214501 (2003).
[14] F. Van der Bos, B. Tao, C. Meneveau, and J. Katz, Phys. Fluids **14**, 2456 (2002).
[15] B. J. Cantwell, Phys. Fluids A **4**, 782 (1992).
[16] V. Borue and S. A. Orszag, J. Fluid Mech. **366**, 1 (1998).
[17] A. Pumir, B. I. Shraiman, and M. Chertkov, Phys. Rev. Lett. **85**, 5324 (2000).
[18] P. Vieillefosse, Physica A **125**, 150 (1984).
[19] A. Pumir, Phys. Fluids **6**, 2071 (1994).
[20] A. Pumir, B. I. Shraiman, and M. Chertkov, Europhys. Lett. **56**, 379 (2001).
[21] W. H. Press, S. A. Teukolsky, W. T. Vetterling, and B. P. Flannery, *Numerical Recipes in C* (Cambridge University Press, Cambridge, 1992).
[22] X. Shen and Z. Warhaft, Phys. Fluids **12**, 2976 (2000).
[23] S. Ayyalasomayajula and Z. Warhaft (private communication).